Hindawi
Advances in Civil Engineering
Volume 2021, Article ID 5685710, 14 pages
https://doi.org/10.1155/2021/5685710

Research Article

An Experimental Study on a Composite Bonding Structure for Steel Bridge Deck Pavements

Xiaoguang Zheng,[1] Qi Ren ,[1] Huan Xiong,[2] and Xiaoming Song[3]

[1]*Shanghai Municipal Engineering Design Institute (Group) Co., Ltd., Shanghai 200092, China*
[2]*Chengdu Xingcheng Construction Management Co., Ltd., Chengdu 610041, China*
[3]*Sika (China) Ltd., Suzhou 215121, China*

Correspondence should be addressed to Qi Ren; qrendavis@gmail.com

Received 22 June 2021; Revised 30 August 2021; Accepted 12 October 2021; Published 26 October 2021

Academic Editor: Xiao Sun

As one of the major contributors to the early failures of steel bridge deck pavements, the bonding between steel and asphalt overlay has long been a troublesome issue. In this paper, a novel composite bonding structure was introduced consisting of epoxy resin micaceous iron oxide (EMIO) primer, solvent-free epoxy resin waterproof layer, and ethylene-vinyl acetate (EVA) hot melt pellets. A series of strength tests were performed to study its mechanical properties, including pull-off strength tests, dumbbell tensile tests, lap shear tests, direct tension tests, and 45°-inclined shear tests. The results suggested that the bonding structure exhibited fair bonding strength, tensile strength, and shear strength. Anisotropic behaviour was also observed at high temperatures. For epoxy resin waterproof layer, the loss of bonding strength, tensile strength, and shear strength at 60°C was 70%, 35%, and 39%, respectively. Subsequent pavement performance-oriented tests included five-point bending tests and accelerated wheel tracking tests. The impacts of bonding on fatigue resistance and rutting propagation were studied. It was found that the proposed bonding structure could provide a durable and well-bonded interface and was thus beneficial to prolong the fatigue lives of asphalt overlay. The choice of bonding materials was found irrelevant to the ultimate rutting depth of pavements. But the bonding combination of epoxy resin waterproof and EVA pellets could delay the early-stage rutting propagation.

1. Introduction

Steel bridge has been playing an important role in civil engineering since the late 19th century. After World War II, an orthotropic system was developed by German engineers driven by the shortage of steel. Bridge decks in this form could possess different stiffness in longitudinal and transverse directions [1], allowing extremely minimized thickness. However, certain distresses could take place due to the flimsy steel deck. One of the most troublesome issues was the failure of overlaying pavement, which was recognized early in 1960s [2]. Cracking on SBDPs appeared much faster than expected, resulting in frequent maintenance and replacement. Two solutions were soon proposed by engineers from north American and Europe, which were known as epoxy asphalt mixture [3, 4] and mastic asphalt mixture [5], respectively. Engineering practice of these solutions turned out to be quite successful across the world [6–9]. Meanwhile, driven by the need of durability and reliability, relevant research was greatly pushed forward. Qian et al. [10] designed a skeleton-dense epoxy asphalt mixture for the purpose of skid resistance and evaluated its performance with a movable accelerated loading simulator (MMLS3). Yin et al. [11] studied the cracking mechanism of epoxy asphalt and recommended epoxy resin-sealing material for SBDP repairing. Widyatmoko et al. [12] demonstrated that the stiffening effect caused by the addition of Trinidad lake asphalt could be altered if proper polymer modifiers were used. Kim et al. [13] evaluated the fatigue performance of styrene-butadiene-styrene (SBS) modified mastic asphalt mixtures by binder tests, four-point bending beam fatigue tests, and indirect strength tests. The SBS modifiers were

found helpful to improve the low temperature crack resistance as well as fatigue life of mastic asphalt. Besides epoxy asphalt and mastic asphalt, stone mastic asphalt (SMA) mixture was another competitive SBDP candidate. A notable advantage of SMA over epoxy asphalt and mastic asphalt was the cost effectiveness. In a typical 2-layer SBDP structure, replacing the upper lift with SMA could achieve a better life cycle cost [14].

The difficulty of SBDP came from the extremely severe conditions on bridges. Traffic load, rain, snow, deicing salt, and even the vibration of the bridge could be a potential threat. Metcalf conducted flexural tests on composite beams to test fatigue performance [15]. The theoretical analysis suggested that large tensile strain might be the cause of short service life. Günther et al. [16] pointed out that damage-level cracks of pavements were related to the structural design of the deck and proposed minimum strength requirements for pavements. In recent years, highly developed finite element modelling software made simulation of SBDP much easier. Kim et al. [17] used a 3-D model to identify key factors affecting the mechanical properties, which turned out to be the maximum transverse tensile strain and interface bonding. Chen et al. [18] used a multiscale numerical model to study crack distribution. It was found that the transverse cracks were a bigger threat than longitudinal cracks. Jia et al. [19] investigated the field performance of two steel bridge pavements by coring and chemical analysis. It was inferred that poor bonding at the interface was the major cause of distresses.

Among all the factors influencing the durability of SBDP, it seemed that the bonding between steel plate and asphalt overlay was the most controllable part. The importance of bonding has been recognized by engineers and researchers for a long time. But limited effort has been made till recent years. Bocci et al. [20] suggested using the physical instead of chemical method to solve the bonding issue by mechanical reinforcement at the interface. The idea of physical reinforcement was possible but unlikely to be favourable by designers or decision makers. Ai et al. [21] tested four different waterproof bonding materials, then developed an entropy-weight Technique for Order Preference by Similarity to an Ideal Solution (TOPSIS) to find the optimal solution based on test results. Zhang et al. [22] studied the adhesion and deformation compatibility issue of epoxy binder and methacrylate acrylate (MMA-) based adhesive. Epoxy binder was found more suitable for epoxy asphalt, while MMA was recommended for mastic asphalt. In addition, the existence of anticorrosive layer was found indispensable. To summarize, the bonding material was supposed to protect the steel plate, prevent moisture infiltration, and maintain a strong adhesion simultaneously. As a result, single material could hardly meet such requirements. Therefore, a composite bonding structure was introduced in this paper. The composite bonding system consisted of 3 parts, a primer based on epoxy resin with micaceous iron oxide (EMIO), a solvent-free epoxy resin waterproof layer, and ethylene-vinyl acetate (EVA) hot melt pellets. Compared with traditional bonding solutions, the following advantageous features made this novel structure a promising candidate to solve the bonding issue: (a) EMIO was used as the primer of steel plate, which could provide fair anticorrosion protection as well as mechanical performance. In all the tests conducted in this study, EMIO was found possessing the greatest bonding strength. (b) In most previous bonding solutions, the waterproof layer served as the bonding material, but the strength was usually not satisfactory. In this study, EVA pellets were placed on top of the waterproof layer to further enhance the bonding. The pellets would melt during the construction period of HMA and form a strong interface. (c) The use of solvent-free epoxy resin was believed to be environmental-friendly compared with traditional waterproof materials.

2. Materials and Test Methods

2.1. Materials. A model of the composite bonding structure was shown in Figure 1.

Corrosion of steel caused by oxidization was theoretically inevitable, but it could be considerably delayed with proper protections. In the proposed bonding structure, EMIO primer was treated as the last defender of the steel plates underneath. Its laminated microstructure could effectively prolong the path of moisture and oxygen infiltration [23]. On top of the primer, solvent-free epoxy resin served as the waterproof layer, inhibiting vertical runoff as well as other detrimental factors, such as dust, oil, and salt. EVA pellets were spread on the surface of the waterproof layer, initially in the state of solid particles. Once hot mixed asphalt (HMA) was paved, the concomitant heat would melt the pellets and eventually form a substantially bonded interface. In this paper, two similar EVA pellets were studied, denoted as "HT" and "LT", respectively. LT was specially designed for cold climate areas, so its melting point was slightly lower than that of HT.

Basically, EMIO, epoxy resin, and EVA were all reliable binders due to their chemical behaviours. To ensure the effect of bonding, the material should reach a certain level to form a thin film covering the interface. This level was determined by a series of tests by the manufacturer for the user's reference, as shown in Table 1. In practice, the usage of bonding material could be adjusted depending on the demand of the users. For example, in the pull-off test in Section 3.1, it was found that further increase of the usage of epoxy resin waterproof material would not significantly strengthen the bonding, but it was beneficial to get more stable test results with less variation.

2.2. Test Methods. As a potential bonding structure for SBDPs, there were more concerns beyond the protection issue of steel plates. Firstly, each material was desired to retain fair adhesion to one another. It would also be beneficial for future maintenance if the weakest spot of the structure could be located. Secondly, the bonding material was expected to bear both tensile and shear stress caused by traffic; thus, the corresponding strengths should be investigated with proper laboratory tests. Thirdly, since most bonding materials had a propensity to soften at high

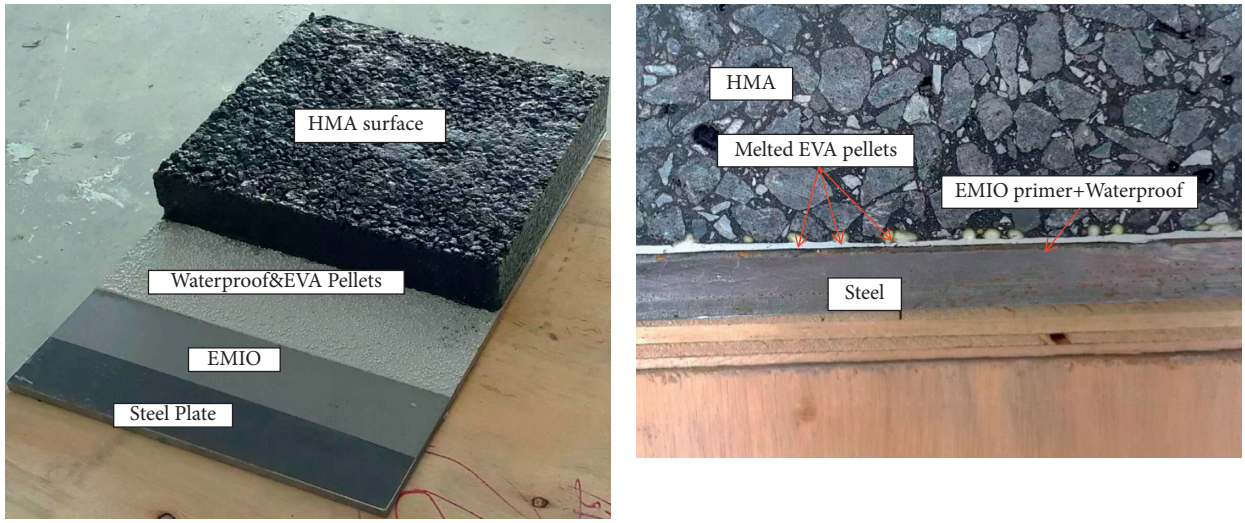

(a) (b)

Figure 1: Composite bonding structure. (a) Structure model and (b) cross section.

Table 1: Material properties of the composite bonding structure [24].

Layer	Material	Density	Recommendation of use
Asphalt overlay			
Hot-melt pellets	EVA	1.2 kg/L	0.7 kg/m^2
Waterproof	Solvent-free epoxy resin	1.7 kg/L	1.7 kg/m^2
Primer	EMIO	1.6 kg/L	0.22 kg/m^2
Steel plate			

temperatures, such conditions should be covered in tests. Lastly, the long-term performance under repeated loading still remained questionable and was worth studying. In light of these considerations, various tests were conducted as listed in Table 2.

Tests 1 to 5 mainly focused on the strength issues of bonding materials, which would be discussed in Section 3. Tests 6 and 7 were pavement performance-oriented tests under simulated traffic loading. They would be discussed in Section 4.

Table 2: Laboratory tests summary.

No.	Concerns	Tests
1	Bonding strength	Pull-off strength test
2	Tensile strength of waterproof layer	Dumbbell tensile test
3	Shear strength of waterproof layer	Lap shear test
4	Structural bonding strength	Direct tension test
5	Structural shear strength	45°-inclined shear test
6	Fatigue behaviour	Five-point bending test
7	Rutting propagation	MMLS3 wheel tracking test

3. Strength-Oriented Tests

3.1. Pull-Off Strength Test. Basically, the proposed bonding structure was likely to fail in three modes: a. EMIO primer stripped of steel, *b*. waterproof separated from EMIO primer, or *c*. overlaying HMA disengaged with waterproof layer. The last debonding mode could hardly be studied without HMA, but the first two modes could be easily tested with pull-off strength tests in accordance with ASTM D 4541-17 [25]. This test would place a metal fixture on top of certain bonding materials. When the material was cured, a portable tester would gradually pull the fixture until detachment, as shown in Figure 2. The maximum stress was recorded as the pull-off strength.

Four groups of pull-off tests were performed. In the first group, EMIO primer was coated on a cleansed steel plate with a density of 0.3 kg/m^2. The second group placed an additional waterproof layer with a density of 3.0 kg/m^2 on top of the EMIO. The third group was similar to the second group but differed in the waterproof density, which was 1.8 kg/m^2. The last group tested another commonly used primer known as Zinc rich epoxy for comparison. The pull-off strength was tested at 3 temperatures of 25°C, 60°C, and 70°C in terms of high-temperature-related softening issues. For each temperature, 4 specimens were tested after 7 days of curing. The test results were plotted in Figure 3.

At 25°C, EMIO primer exhibited the highest values among all specimens. In contrast, zinc rich epoxy primer was 54.6% smaller. Meanwhile, introduction of waterproof layer could significantly decrease the bonding strength of the structure. Photos of failed specimens were shown in Figure 4. Comparing the failure mechanism in Figure 4(a) and

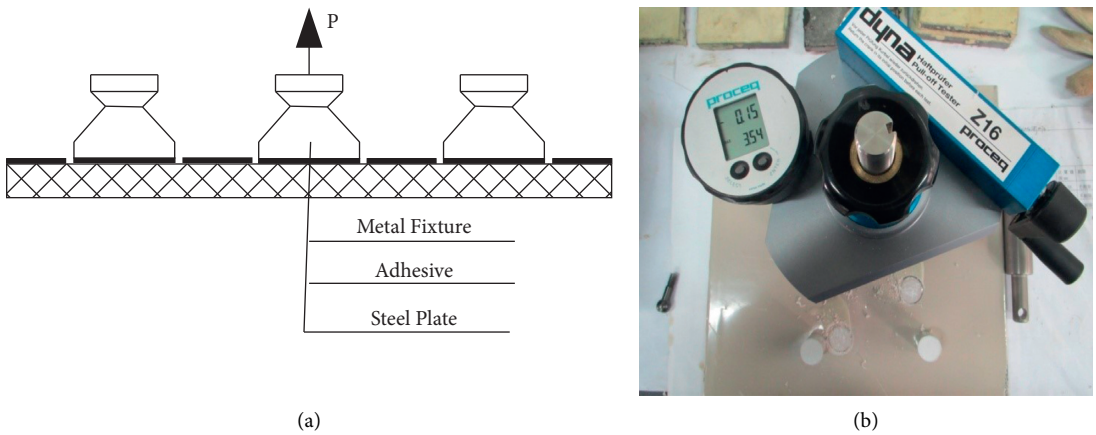

(a) (b)

Figure 2: Pull-off adhesion strength test. (a) Schematic diagram of the test. (b) Photo of a portable adhesion tester.

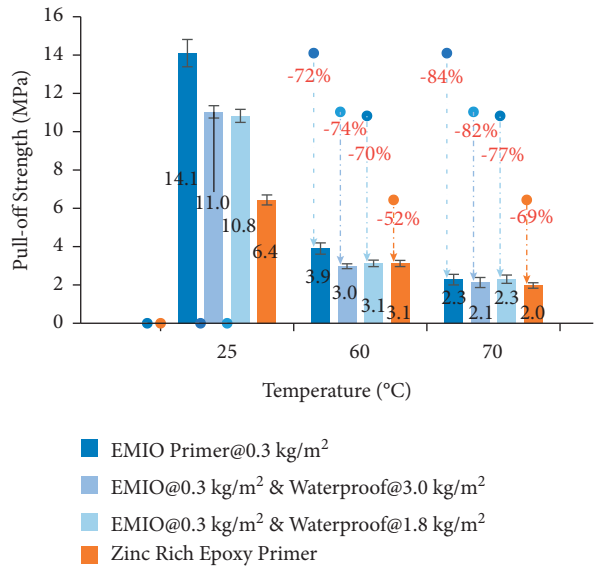

Figure 3: Pull-off strength test results.

(a) (b)

Figure 4: Failure photos of pull-off tests. (a) Failure at EMIO-steel interface (25°C). (b) Failure at waterproof-EMIO interface (25°C, 3.0 kg/m^2).

Figure 4(b), it could be seen that debonding between waterproof material and EMIO could occur prior to the detachment of EMIO and steel plate. Similar failure mode was also observed under the other test conditions. Thus, it could be inferred that the waterproof-EMIO bonding was much weaker than that of the EMIO-steel bonding. As the temperature raised, significant loss of strength could be found in all specimens. At 60°C and 70°C, EMIO primer could lose 72.3% and 82.5% of its strength, respectively. For waterproof layer at the same temperatures, the strength losses were 72% and 80% in average. It should be noted that the different densities of the waterproof layer did not remarkably alter the bonding strength. A plausible explanation for this phenomenon was that the density of 1.8 kg/m^2 was sufficient to form a thin film on the surface, and merely increasing the thickness of that film would not help better bonding of the interface. However, a higher density of 3.0 kg/m^2 was still preferred in laboratory studies because it could guarantee more stable test results.

3.2. Tensile Strength Test. Epoxy resin waterproof material was placed under the HMA overlay. Under traffic load, it is likely to bear tensile stress. Dumbbell tensile test in accordance with ASTM D 638-14 [26] was adopted to investigate its mechanical properties. Details of the test were exhibited in Figure 5. Epoxy resin specimens were prepared in a dumbbell-shaped mold with a thickness of 3.5 mm. When the specimens were cured, they were gripped by the tester at each end and then stretched at a constant speed of 500 ± 5 mm/min till failure. The maximum stress during the test was recorded as the tensile strength.

Two groups of specimens were prepared for tests after 7 days curing. The test temperatures were set to 25°C and 60°C. The test results were plotted in Figure 6. At 25°C, the waterproof layer exhibited typical elastic-plastic behaviours and yielded stress before breaking. The tensile strength was over 10 MPa, which was adequate in most cases. The average elongation rate of 16.1% also suggested fair ductility. At 60°C, the strength dropped approximately by 35%, but the specimen was not breaking during the test. This implied that the tested tensile strength was not actually representing the yielding stress, and the result was thus considered conservative. Tests at 70°C were therefore unnecessary since the exact tensile stress at such conditions would be unknown in this test mode.

3.3. Lap Shear Test. Besides tension, shear was another consideration for bonding material in structural design. Lap shear tests were adopted based on ASTM D 1002-10 [27] in this study. The test procedures were shown in Figure 7. Firstly, two steel plates were cleansed at one end and coated with EMIO. After 1 day of curing, the coated ends were overlapped and glued together by a membrane of epoxy resin waterproof layer. The curing time for assembled specimens was 7 days. Afterwards the tester would apply tension from each end, causing a shear stress within the membrane. The maximum shear stress during the test was recorded as the shear strength.

Lap shear tests were conducted at temperatures of 25°C, 60°C, and 70°C. The test results were plotted in Figure 8. Judging from Figure 7(c), it could be seen that the waterproof layer failed due to shear, but the bonding between steel and EMIO remained intact. This phenomenon implied that the bonding provided by the waterproof layer was weaker than that of EMIO primer, which was identical with previous test results. Another notable fact was the anisotropic behaviour of waterproof material under high temperature conditions. At 60°C, the loss of bonding strength was approximately 70%. Meanwhile tensile and shear strength were only decreased by 35% and 39%, respectively. It could be inferred that the temperature-induced softening mechanism would trigger debonding issues prior to the failure caused by shear or tension.

3.4. Direct Tension Test. The bonding effect between waterproof and HMA overlay was determined by two critical factors. The first one was the strength provided by the bonding material, which was thoroughly studied by researchers. But the other factor could be easily ignored, which was the contact area. Air voids existed in HMA even if the best compaction was performed. The substantially contacted area was thus smaller than the paving area. For SBDPs, the situation could be worse because the compaction effort was likely to be restricted. The introduction of EVA pellets was targeted on this issue. When the pellets were melted and able to flow, they could be squeezed into the HMA voids by compaction. This mechanism not only provided extra bonding by enlarging the contact area but also enhanced the structural integrity by coarsening the interface.

In this study, direct tension tests were employed to study the bonding between waterproof and HMA overlay, as shown in Figure 9. Asphalt mixture used in this test was stone mastic asphalt (SMA), a commonly used gap-graded mixture. For test setup, EMIO primer was coated on a 10 cm × 10 cm steel plate first. Epoxy resin waterproof and EVA pellets were then placed with densities of 3.0 kg/m^3 and 0.8 kg/m^3. After the waterproof layer was cured, a 4 cm SMA lift was paved to melt the pellets. The other end of the specimen was glued to an identical steel plate with fast-setting epoxy resin. The assembled specimen would be stretched by the tester at a constant speed of 10 mm/min until failure.

Two kinds of EVA pellets, HT and LT, were tested at three different temperatures of 25°C, 60°C, and 70°C, respectively. The melting temperature of LT was slightly lower, which made it a potential candidate for cold area or warm mixed conditions. Test results are summarized in Figure 10. At 25°C and 60°C, SMA failed prior to the interface. The tested strength actually belonged to SMA instead of the bonding structure. Thus, only the test results at 70°C could properly represent the bonding strength. The combination of different pellets showed no significant compact on test results. It could be inferred that the bonding provided by either structure was stronger than HMA tensile strength at low temperatures. Potential debonding distress only took place at extremely high temperature conditions.

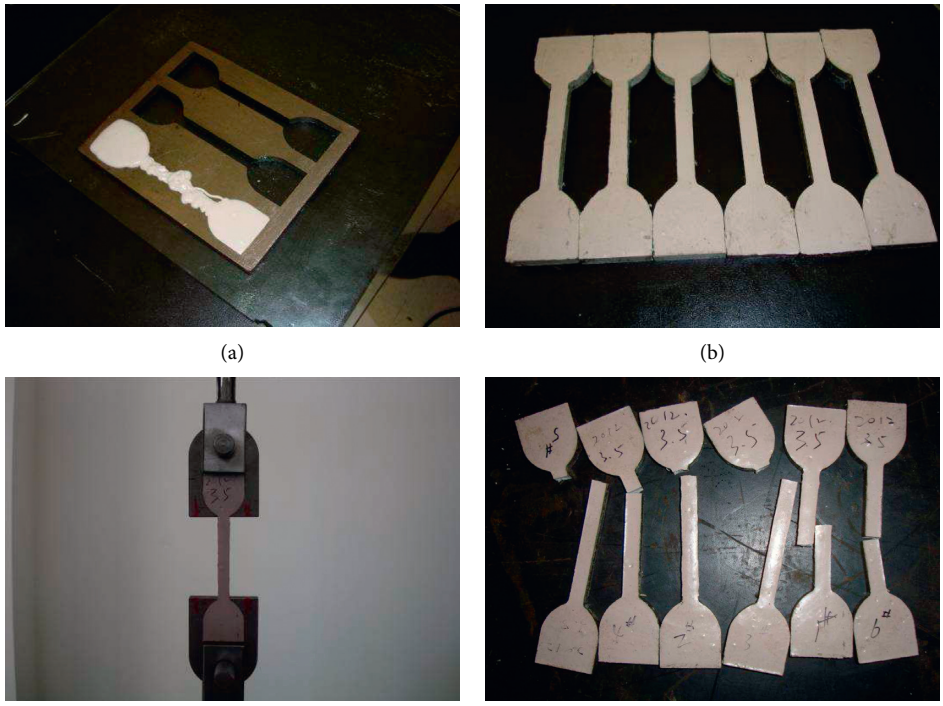

Figure 5: Dumbbell tensile test. (a) Dumbbell-shaped mold for specimen preparation; (b) dumbbell-shaped specimens; (c) tensile test apparatus; and (d) failed specimens.

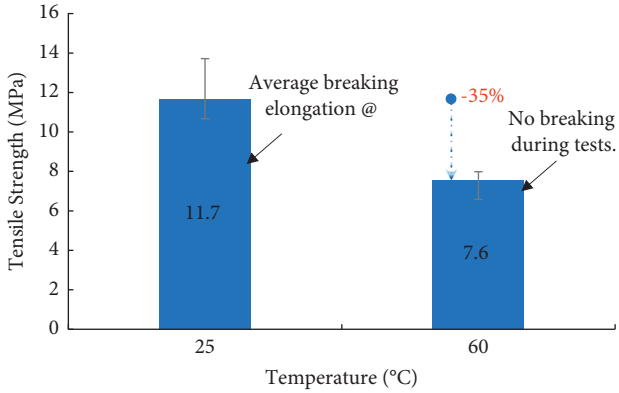

Figure 6: Dumbbell tensile strength test results.

3.5. Inclined Shear Test. The shear strength provided by EVA pellets was investigated by 45°-inclined shear tests, as shown in Figure 11. The specimen preparation was similar to that of direct tension test, except that it was placed 45° off the horizontal plane. The tester applied a compressive load in the vertical direction, causing a shear stress along the interface.

An alternative option was direct shear test [28]. These two methods differed only in how the normal stress was applied at the interface. For direct shear test, the normal stress could be altered manually, allowing for a wide range of different stress states to be tested and thus quite suitable for the establishment of constitutive equations. In contrast, inclined shear test maintained a constant normal-shear stress ratio, and the shear strength results were found more stable in practice.

8 groups of specimens were tested at three temperatures of 25°C, 60°C, and 70°C. The first group was tested at the standard condition. The interface was bonded with waterproof and HT pellets at densities of 3.0 kg/m2 and 0.8 kg/m2, while SMA overlay was compacted at 170°C. The 2nd to 4th groups altered the density settings in order to study the impact if less bonding material was used in construction. The 5th to 8th groups introduced LT pellets as well as lower compaction temperature of 150°C. In all tests, the specimens failed due to SMA-waterproof interface detachment. The test results are plotted in Figures 12 and 13.

Judging from Figure 12, changing the densities of waterproof or HT pellets could hardly result in fluctuations of shear strength. The loss of shear strength at 60°C and 70°C was approximately 74% and 85% in average, respectively. It

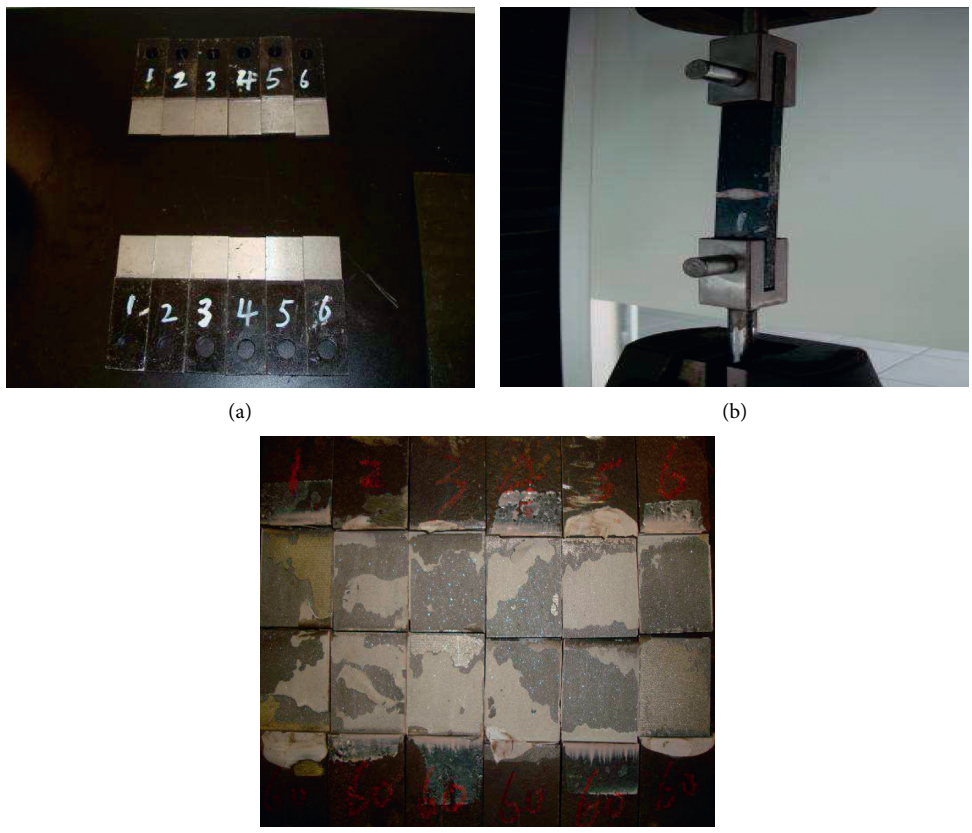

Figure 7: Lap shear test. (a) Specimen preparation; (b) test setup; and (c) failed specimens after test.

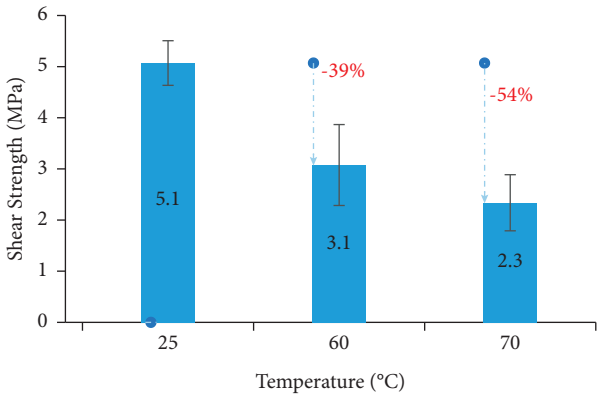

Figure 8: Lap shear test results.

should also be noted that these values were closer to the results of EMIO-waterproof pull-off tests instead of lap shear test. A plausible explanation for this phenomenon was that the temperature-induced softening mechanism would most significantly weaken the bonding strength. As a result, the interface detached due to shear prior to the failure of waterproof membrane or SMA.

In construction phase, the control of compaction temperature could not be as perfect as laboratory conditions. In some cases, warm mixed asphalt could also be used due to aging or environmental considerations. The tests on LT pellets and lower compaction temperature aimed to investigate such influence. It could be seen from Figure 13 that the 150°C-compaction temperature could undermine the structural shear strength of HT pellets structure at a magnitude of 5%, 43%, and 31% at 25°C, 60°C, and 70°C, respectively. Clearly such impact was more significant at high temperatures. As for LT pellets, the strength at 25 °C was 7% higher than that of HT under 170°C-compaction. However, LT-structure could lose 88% and 94% of its strength at 60°C and 70°C, respectively, which made its performance worse than HT-structure at such temperatures. Meanwhile, lower compaction temperature could scarcely influence the LT-structure. This was likely to be caused by its lower melting point. Therefore, the trade-off of LT pellets was that it partly sacrificed high temperature performance in exchange for compatibility of lower compaction temperature.

It could be seen from the strength-oriented test results that the strength provided by bonding materials was greater than that of HMA overlay at 25°C, in both shear or tensile modes. The only strength-related concern was the high temperature conditions. Due to the chemical properties, the bonding materials would soften faster than asphalt mixture. This phenomenon could result in a faster deterioration in practice and should be considered in design stage. Besides the strength issues, the performance under repeated loading remained another crucial consideration, which would be investigated in the following section.

Figure 9: Direct tension test. (a) Specimen preparation. (b) Test setup. (c) Failure of SMA (25°C and 60°C). (d) Interface debonding (70°C).

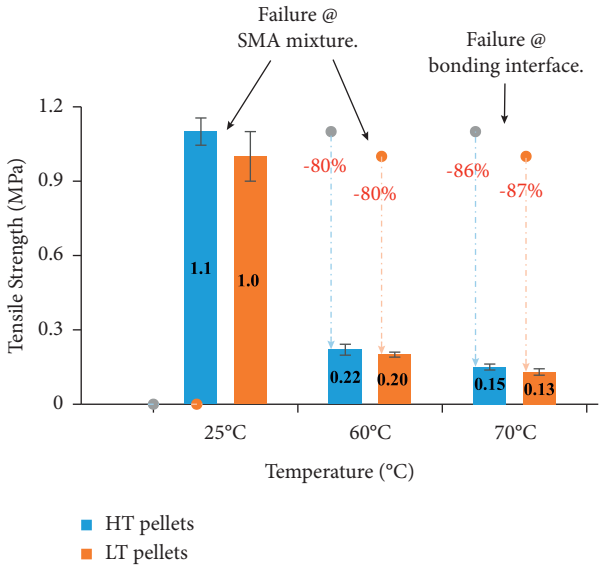

Figure 10: Direct tension test results.

(a) (b)

Figure 11: Inclined shear test. (a) Test setup. (b) Failed interface.

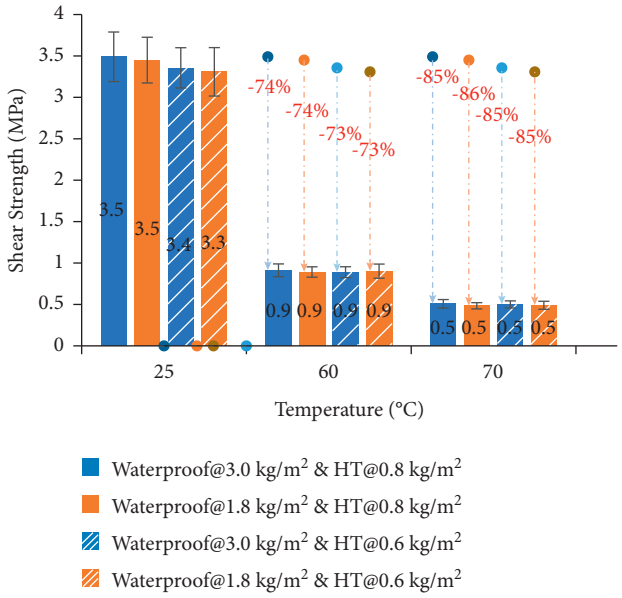

Figure 12: Inclined shear test results in terms of different material densities.

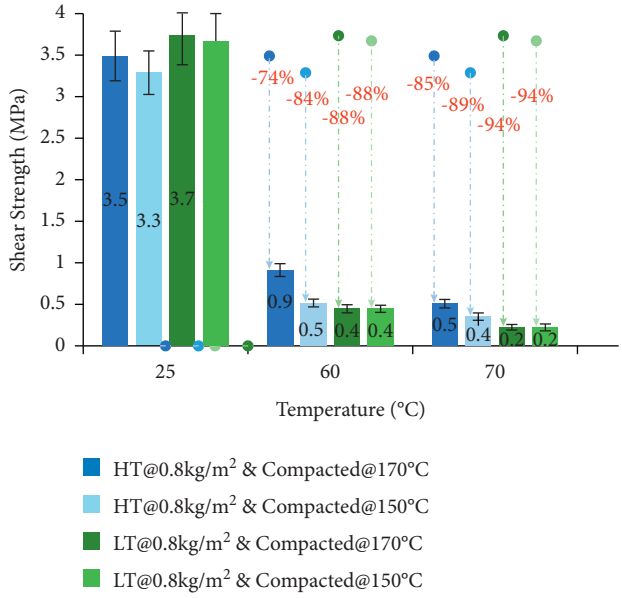

Figure 13: Inclined shear test results in terms of different pellets and compaction temperatures.

4. Pavement Performance-Oriented Tests

4.1. Five-Point Bending Test. To study the fatigue resistance of SBDP, five-point bending test (FPBT) was adopted. In Figure 14 FPBT would cause a negative moment in the centre of the beam [29]. Liu et al. used a 3-D finite element model to simulate asphalt overlay on orthotropic steel decks and strongly recommended FPBT as an ideal test method for this issue [30]. A sketch of FPBT test is shown in Figure 14(a). The specimen of FPBT was a 700 mm × 200 mm×12 mm steel plate with a 700 mm × 150 mm×40 mm asphalt overlay. This composite beam was supported by 3 rollers at offsets of 50 mm, 350 mm, and 650 mm, respectively, while the load was applied symmetrically at the locations of 175 mm and 525 mm. The specimens were tested in stress-controlled mode to simulate real traffic conditions at 20°C. A sinuous load ranging from 2.7 kN to 18 kN with a frequency of 10 Hz was determined based on trial loadings.

The specimen preparation of FPBT is shown in Figure 14(b). First a steel plate was coated with primer and waterproof layer. Then a rectangular mold was placed on top of it. HMA overlay would be filled in the mold and compacted with a slab roller. When the temperature of HMA was cool enough, the mold could be removed and the beam specimen was placed in the test equipment. Four linear variable differential transformers (LVDTs) were fixed on top of the surface to monitor the tensile strains, as shown in Figure 14(c).

Four groups of FPBTs were conducted as shown in Table 3. Three parallel specimens were tested for each group. For all tests, the steel plates underneath were coated with EMIO primer. The 1st group consisted of SMA overlay and

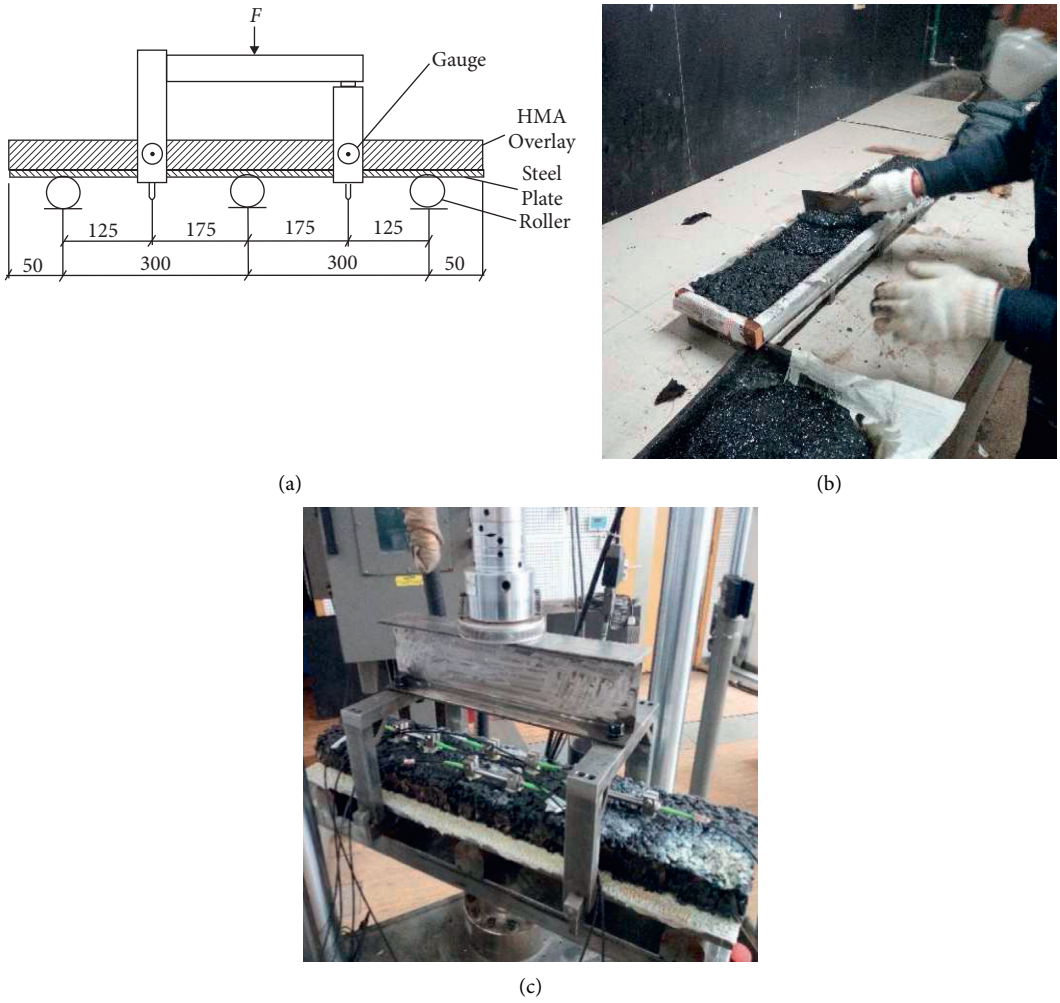

Figure 14: Five-point bending test setup. (a) Sketch of FPBT. (b) Specimen preparation. (c) LVDT setup.

Table 3: Pavement structures for FPBT.

Structure no.	1	2	3	4
HMA overlay	SMA	GA	SMA	SMA
Interface bonding	HT pellets and epoxy resin	HT pellets and epoxy resin	Epoxy resin	Rubberized asphalt
Steel plate + EMIO primer				

the standard bonding structure proposed in this paper, which was the combination of HT pellets and solvent-free epoxy resin waterproof material. In the 2nd group, SMA was replaced with Guss-asphalt mixture (GA). The 3rd and 4th groups both employed SMA overlay but differed in the interface bonding. The 3rd group removed HT pellets from the structure and used epoxy resin alone, while the 4th group adopted rubberized asphalt waterproof material.

For stress-controlled fatigue test, the modulus of specimen would gradually decrease as the microcracks accumulated in the structure. As a result, increasing tensile strain could be observed with the loading repetition. As the microcracks grew and merged to form fractures in the beam, eventually the specimen would not be able to stand the load anymore and the LVDTs would observe an extremely large strain exceeding the range. This point was defined as fatigue failure, and the corresponding loading repetition was defined as fatigue life. In this study, when the loading repetition reached 1 million, the load was increased by 50% to accelerate failure. The tensile strains in the centre of the beam during the tests are plotted in Figure 15.

In terms of asphalt overlays, GA maintained a smaller tensile strain during the test compared with SMA overlays. The selection of bonding materials could also result in different fatigue behaviours. The combination of HT pellets and epoxy resin waterproof layer excelled rubberized asphalt in fatigue resistance with both smaller tensile strain and longer fatigue life. However, removing HT pellets from the bonding structure would increase the surface tensile strain by 20% and lead to much earlier failure. The performance of

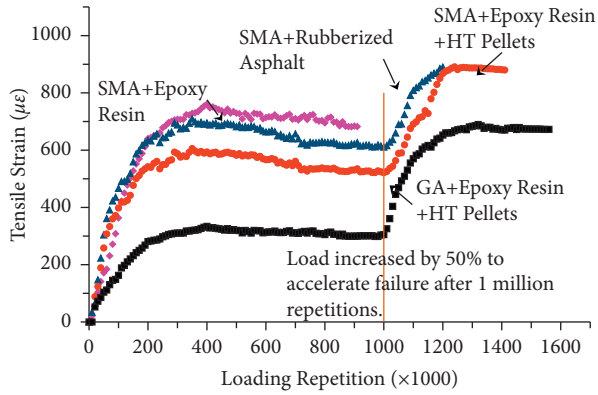

Figure 15: FPBT fatigue test results.

(a) (b)

Figure 16: MMLS3 apparatus. (a) Overview. (b) Water channel for specimens.

Table 4: Specimen preparation for accelerated pavement test.

Specimen	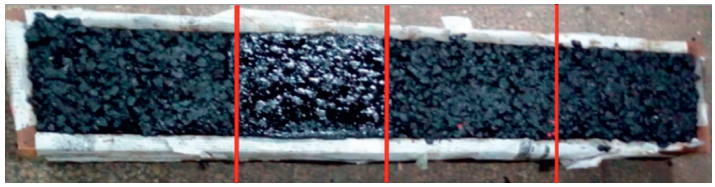			
Length	22.5 cm	22.5 cm	22.5 cm	22.5 cm
Surface HMA	SMA	GA	SMA	SMA
Interface bonding	HT pellets and epoxy resin	HT pellets and epoxy resin	Rubberized asphalt	Epoxy resin
	Steel plate + EMIO primer			

epoxy resin waterproof material alone was worse than that of rubberized asphalt. This phenomenon further validated the effectiveness of EVA pellets.

4.2. Accelerated Wheel Tracking Test. Permanent deformation was another major distress of pavements. In this study, a one-third scale Model Mobile Load Simulator (MMLS3) was used to study the rutting resistance, as shown in Figure 16. The advantage of this simulator on rutting evaluation was validated by Epps et al. [31] at WesTrack. In recent years, MMLS3 was also preferred by researchers in rutting-related studies due to its efficiency and convenience [32].

The specimen was fabricated as shown in Table 4. The total length of the specimen was 900 mm and was equally assigned to 4 sections. The combinations of asphalt overlays and bonding materials were consistent with that of FPBT fatigue tests. The 6 cm-thick specimen was then bathed in 60°C-water to accelerate rutting propagation. The loading system applied channelized loads with rubber tires at a magnitude of 50 kN and a tire pressure of 700 kPa at a frequency of 5000 times/hr.

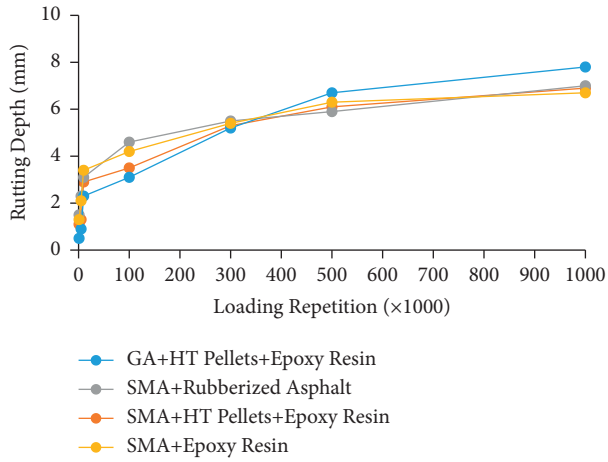

Figure 17: Rutting propagation in accelerated pavement test.

During the test, no stripping or interface detachment was observed. The cumulative rutting depths at 1 k, 100 k, 300 k, 500 k, and 1000 k repetitions were measured and plotted in Figure 17. The rutting of GA was smaller than that of SMA before 300 k repetitions, but its ultimate depth was the greatest. A possible explanation was that the absence of compaction weakened the rutting resistance of GA. As for SMA, the rutting depth in early stage showed certain difference. The performance of the section using HT pellets and epoxy resin was the best while rubberized asphalt section was the worst. However, the ultimate rutting depth of all SMA sections converged to approximately 7 mm after 1 million loading repetitions. It could be thus inferred that the bonding material selection had little impact on the final rutting depth, but using the combination of EVA pellets and epoxy resin waterproof material could effectively delay rutting propagation in early stages. This conclusion was also conservative because the factor of asphalt aging could not be incorporated in accelerated tests.

5. Conclusions

This paper introduced a novel bonding structure for SBDP, consisting of EMIO primer, solvent-free epoxy resin waterproof layer, and EVA hot melt pellets. Various laboratory tests were conducted to study its performance in terms of strength as well as resistance to fatigue and rutting. In terms of the test results, some key findings were summarized as follows.

(a) In the pull-off tests, bonding strengths of steel-EMIO and EMIO-waterproof were tested. The performance of EMIO primer was satisfactory. In subsequent tests, EMIO primer was never found to strip or fail. The EMIO-waterproof interface was believed to be a potential weak spot in the structure. Its bonding strength was 20% smaller than that of steel-EMIO interface at 25°C. A waterproof density of 1.8 kg/m^2 was sufficient to provide fair bonding. Further raising the density would not significantly enhance the strength but could achieve smaller deviation in tests.

(b) The tensile strength and shear strength of solvent-free epoxy resin waterproof coating were tested with dumbbell tensile test and lap shear test, respectively. The epoxy resin was found to be anisotropic at high temperatures. The loss of bonding strength, tensile strength, and shear strength at 60°C was approximately 70%, 35%, and 39%, respectively. High temperature conditions would likely to cause debonding prior to other distresses.

(c) Two kinds of EVA pellets were adopted in the bonding structure aiming to further enhance the bonding between epoxy resin waterproof and HMA overlay. Such bonding was tested with direct tension tests. At 25°C and 60°C, HMA failed prior to the bonding structure, so it could be inferred that the bonding strength was sufficient for both pellets.

(d) A series of 45°-inclined shear tests were conducted to identify the key contributors to shear strength. For HT pellets, varying the densities of epoxy resin waterproof layer or the pellets could hardly cause strength fluctuation. But the compaction temperature of HMA overlay was critical. The 150°C-compaction condition could result in a 43% shear strength loss at 60°C. For LT pellets, its 25°C-shear strength as well as its tolerance with lower compaction temperature was better compared with HT. However, its strengths at 60°C and 70°C were only 50% of those of HT pellets.

(e) In FPBT fatigue tests, the bonding combination of epoxy resin waterproof layer and HT pellets exhibited the minimum tensile strain as well as the longest fatigue life. However, once HT pellets were removed from the structure, the tensile strain could increase by 20% instantly and result in a much sooner failure of the specimen.

(f) Rutting behaviours were tested with MMLS3 accelerated wheel tracking test. It was found that the

ultimate rutting depth after 1 million loading repetition was irrelevant with the bonding materials. However, the combination of epoxy resin waterproof and HT pellets could effectively delay rutting propagation in early stages.

To conclude, the overall performance of the proposed bonding structure was satisfactory in both strength tests and pavement performance tests. Its application was believed to be promising. A major limitation was that its engineering practice would require a highly skilled construction team, strict obedience to the technique protocols, and well-organized supervision. In relevant pilot projects, it was noticed that poor management could result in a disastrous construction quality. Future study would mainly focus on its field performance and maintenance issues.

Data Availability

The data used to support the findings of this study are available from the corresponding author upon request.

Conflicts of Interest

The authors declare that there are no conflicts of interest regarding the publication of this paper.

Acknowledgments

The authors would like to express gratitude to Sika (China) Ltd. for their support. This research was funded by Chengdu Xingcheng Construction Management Co., Ltd. (no. K2020K180B-01).

References

[1] A. R. Mangus and S. Sun, "Ch. 14: orthotropic deck bridges," in *Bridge Engineering Handbook*, W.-F. Chen and L. Duan, Eds., , CRC Press, Boca Raton Fl, USA, 1st edition, 1999, ISBN 0-8493-7434-0.

[2] F. N. Finn, "Factors Involved in the design of asphalt pavement surfaces," *The National Co-operative Highway Research Program*, NCHRP Rep. No. 39, Transportation Research Board, Washington, D.C, USA, 1967.

[3] B. Balala, "First orthotropic bridge deck paved with epoxy asphalt, (San Mateo-Haywood)," *Civil Engineering ASCE*, vol. 38, no. 4, p. 59, 1968.

[4] B. Balala, "Studies leading to choice of epoxy asphalt for pavement on steel orthotropic bridge deck of san mateo-hayward bridge," *Highway Research Record*, vol. 287, pp. 12–18, 1969.

[5] S. Luo, Z. Qian, X. Yang, and H. Wang, "Design of gussasphalt mixtures based on performance of gussasphalt binders, mastics and mixtures," *Construction and Building Materials*, vol. 156, pp. 131–141, 2017.

[6] J. J. Rebbechi, "Epoxy asphalt surfacing of west gate bridge," in *Proceedings of the Australian Road Research Board (ARRB) Conference, 10th*, no. 3, Sydney, August 1980.

[7] W. Huang, Z. Qian, G. Chen, and J. Yang, "Epoxy asphalt concrete paving on the deck of long-span steel bridges," *Chinese Science Bulletin*, vol. 48, no. 21, pp. 2391–2394, 2003.

[8] I. J. Dussek and M. Sida, "The surfacing of two major asian suspension bridges," *The Asphalt Yearbook*, Institute of Asphalt Technology, Middlesex, UK, 1999.

[9] G. Zou, X. Xu, J. Li, H. Yu, C. Wang, and J. Sun, "The effects of bituminous binder on the performance of gussasphalt concrete for bridge deck pavement," *Materials*, vol. 13, no. 2, p. 364, 2020.

[10] Z.-d. Qian, Y. Liu, C.-b. Liu, and D. Zheng, "Design and skid resistance evaluation of skeleton-dense epoxy asphalt mixture for steel bridge deck pavement," *Construction and Building Materials*, vol. 114, pp. 851–863, 2016.

[11] C. Yin, H. Zhang, and Y. Pan, "Cracking mechanism and repair techniques of epoxy asphalt on steel bridge deck pavement," *Transportation Research Record: Journal of the Transportation Research Board*, vol. 2550, no. 1, pp. 123–130, 2016.

[12] I. Widyatmoko, R. C. Elliott, and J. M. Read, "Development of heavy-duty mastic asphalt bridge surfacing, incorporating Trinidad Lake asphalt and polymer modified binders," *Road Materials and Pavement Design*, vol. 6, no. 4, pp. 469–483, 2005.

[13] T. W. Kim, J. Baek, H. J. Lee, and J. Y. Choi, "Fatigue performance evaluation of SBS modified mastic asphalt mixtures," *Construction and Building Materials*, vol. 48, pp. 908–916, 2013.

[14] D. Zhang, F. Ye, and J. Yuan, "Life-cycle cost analysis (LCCA) on steel bridge pavement structural composition," *Procedia - Social and Behavioral Sciences*, vol. 96, pp. 785–789, 2013.

[15] C. T. Metcalf, "Flexural tests of paving materials for orthotropic steel plate bridges," *Highway Research Record*, vol. 155, 1967.

[16] G. H. Günther, S. Bild, and G. Sedlacek, "Durability of asphaltic pavements on orthotropic decks of steel bridges," *Journal of Constructional Steel Research*, vol. 7, no. 2, pp. 85–106, 1987.

[17] T. W. Kim, J. Baek, H. J. Lee, and S. Y. Lee, "Effect of pavement design parameters on the behaviour of orthotropic steel bridge deck pavements under traffic loading," *International Journal of Pavement Engineering*, vol. 15, no. 5, pp. 471–482, 2014.

[18] L. Chen, Z. Qian, and J. Wang, "Multiscale numerical modeling of steel bridge deck pavements considering vehicle–pavement interaction," *International Journal of Geomechanics*, vol. 16, no. 1, Article ID B4015002, 2016.

[19] X. Jia, B. Huang, S. Chen, and D. Shi, "Comparative investigation into field performance of steel bridge deck asphalt overlay systems," *KSCE Journal of Civil Engineering*, vol. 20, no. 7, pp. 2755–2764, 2016.

[20] E. Bocci and F. Canestrari, "Analysis of structural compatibility at interface between asphalt concrete pavements and orthotropic steel deck surfaces," *Transportation Research Record: Journal of the Transportation Research Board*, vol. 2293, no. 1, pp. 1–7, 2012.

[21] C. Ai, H. Huang, A. Rahman, and S. An, "Establishment of a new approach to optimized selection of steel bridge deck waterproof bonding materials composite system," *Construction and Building Materials*, vol. 264, Article ID 120269, 2020.

[22] M. Zhang, P. Hao, G. Men, N. Liu, and G. Yuan, "Research on the compatibility of waterproof layer materials and asphalt mixture for steel bridge deck," *Construction and Building Materials*, vol. 2020, Article ID 121346, 2020.

[23] B. Nikravesh, B. Ramezanzadeh, A. A. Sarabi, and S. M. Kasiriha, "Evaluation of the corrosion resistance of an epoxy-polyamide coating containing different ratios of

micaceous iron oxide/Al pigments," *Corrosion Science*, vol. 53, no. 4, pp. 1592–1603, 2011.

[24] Sika Industry, June 2nd, 2021, https://industry.sika.com/en/products.html.

[25] Astm Standard D4541, 2017, *Standard Test Method for Pull-Off Strength of Coating Using Portable Adhesion Testers*, ASTM International, West Conshohocken, PA, 2017, http://www.astm.org.

[26] Astm Standard D638, 2014, *Standard Test Method for Tensile Properties of Plastics*, ASTM International, West Conshohocken, PA, 2014, http://www.astm.org.

[27] Astm Standard D1002, 2010, *Standard Test Method for Apparent Shear Strength of Single-Lap-Joint Adhesively Bonded Metal Specimens by Tension Loading (Metal to Metal)*, ASTM International, West Conshohocken, PA, 2019, http://www.astm.org.

[28] B. Yao, F. Li, X. Wang, and G. Cheng, "Evaluation of the shear characteristics of steel-asphalt interface by a direct shear test method," *International Journal of Adhesion and Adhesives*, vol. 68, pp. 70–79, 2016.

[29] A. Houel and L. Arnaud, "A five point bending test for asphalt cracking on steel plates," *Pavement Cracking: Mechanisms, Modeling, Detection, Testing and Case Histories*, vol. 261, 2008.

[30] X. Liu, J. Li, G. Tzimiris, and T. Scarpas, "Modelling of five-point bending beam test for asphalt surfacing system on orthotropic steel deck bridges," *International Journal of Pavement Engineering*, vol. 2019, Article ID 1697440, 22 pages, 2019.

[31] A. L. Epps, T. Ahmed, D. C. Little, M. Y. Mikhail, and F. Hugo, "Performance assessment with the MMLS3 at westrack (with discussion)," *Journal of the Association of Asphalt Paving Technologists*, vol. 70, 2001.

[32] J. Lee, Y. R. Kim, and J. Lee, "Rutting performance evaluation of asphalt mix with different types of geosynthetics using MMLS3," *International Journal of Pavement Engineering*, vol. 16, no. 10, pp. 894–905, 2015.